Materials Advances

ROYAL SOCIETY OF CHEMISTRY

PAPER

View Article Online
View Journal | View Issue

Cite this: *Mater. Adv.*, 2020, 1, 2339

ZnO nanostructures: a heterogeneous catalyst for the synthesis of benzoxanthene and pyranopyrazole scaffolds *via* a multi-component reaction strategy†

Prakash Chhattise,*[ab] Suheb Saleh,[c] Vikram Pandit,[b] Sudhir Arbuj[d] and Vasant Chabukswar*[a]

Received 10th June 2020,
Accepted 21st August 2020

DOI: 10.1039/d0ma00403k

rsc.li/materials-advances

A hydrothermal technique is employed for the preparation of nanostructured ZnO. The reaction was carried out at 180 °C for 2 h in the presence of ethylenediamine (EDA) as a capping agent and was characterized by X-ray diffraction (XRD), scanning electron microscopy (FESEM), and transmission electron microscopy (TEM). XRD indicates the formation of highly crystalline ZnO having a wurtzite structure. FESEM analysis validates the formation of a submicron size spherical shaped marigold flower like morphology. The nanostructured ZnO was screened for its catalytic activity as a heterogeneous catalyst for the multicomponent synthesis of benzoxanthenes and pyranopyrazole derivatives in good to excellent yield. The major advantages associated with this methodology include ease of separation and reusability of the catalyst, easy work-up and short reaction time.

Introduction

Multi-component reactions (MCRs) play an important role in total synthesis and combinatorial chemistry because of their ability to synthesize heterocyclic scaffolds with numerous degrees of structural diversity. Such reactions have received considerable attention because of their simplicity and economical aspects that allow chemists to explore the synthesis of structurally diverse organic compounds.[1] The nanostructured metal oxides such as ZnO, CuO, MgO, TiO_2 Fe_2O_3 *etc.* have attracted much attention due to their unique properties which offer greater surface-to-volume ratio and higher catalytic activity.[2]

Synthesis of heterocyclic compounds has received substantial attention due to their wide range of pharmacological and biological applications. The benzoxanthenes are a very important class of biologically active heterocyclic compounds in medicinal fields. They exhibit mainly anti-inflammatory, antiviral and antibacterial activities.[3–5] They can also be used as dyes,[6] pH-sensitive fluorescent materials for the visualization of bimolecular assemblies[7] and laser technologies.[8] Numerous methods have been reported for the synthesis of benzoxanthene derivatives, which include trontiumtriflate,[9] silicasulphuricacid,[10] P_2O_5 and indium(III) chloride,[11,12] methane sulfonic acid,[13] $NaHSO_4$–SiO_2,[14] *p*-dodecylbenzenesulfonic acid (DBSA),[15,16] tetrabutylammonium-hydrogensulphate (TBAHS).[17] imidazolium based ionic liquid [bmim]PF_6,[18] and trimethylsilyl chloride (TMSCL).[19] Pyranopyrazole derivatives are a significant class of biologically active heterocycles. They exhibit various biological activities such as anticancer, antimicrobial, analgesic, anti-inflammatory, mollucicidal and fungicidal activities. These derivatives are also used as cosmetics and pigments.[20–24] Various methods have been reported for the synthesis of these derivatives such as Prolinetriflate,[25] PTSA in ionic liquid,[26] magnetic nano particle supported dual ionic liquid 3-sulfobutyl-1-(3-propyltriethoxysilane)imidazolium hydrogen sulfate/SiO_2–Fe_3O_4.[27] Nanocrystalline ZnO,[28] and basic ionic liquids.[29] Although the traditional synthetic methodologies offer efficiency, most of them suffer from certain limitations such as low yields of the products, use of harsh reaction conditions, toxic solvents and catalysts compared to nanostructured materials. The semiconducting material ZnO in its nanostructured form has been extensively used in a wide range of technological applications such as electrical engineering, photodegradation of microorganisms, catalysis, and optical and optoelectronic devices.[30–36] In the present work nanostructured ZnO is utilized as a heterogeneous catalyst in multi-component organic transformations and can be used for the formation of binary or ternary composite nanomaterials for a variety of applications.[37,38] In this

[a] *Department of Chemistry, Ness Wadia Nanomaterial Research Centre, NowrosjeeWadia College (Affiliated to SavitribaiPhule Pune University), Pune, India. E-mail: pk3600se@gmail.com*
[b] *Department of Chemistry, Haribhai V. Desai Collge, (Affiliated to SavitribaiPhule Pune University), Pune-411002, India*
[c] *Ministry of Education, Outstanding Secondary School, Iraq*
[d] *Materials for Renewable Energy Division, Centre for Materials for Electronics Technology, Off Pashan Road, Panchwati, Pune-411008, India*
† Electronic supplementary information (ESI) available. See DOI: 10.1039/d0ma00403k

regard, we have developed a simple, efficient, non-toxic heterogeneous catalytic system for the multi-component synthesis of heterocyclic scaffolds like benzoxanthene and pyranopyrazole derivatives *via* one pot four component reactions.

Experimental

Materials and reagents

For the synthesis of ZnO nanostructures, zinc nitrate ($Zn(NO_3)_2 \cdot 6H_2O$), sodium hydroxide (NaOH), and ethylenediamine (EDA) of analytical grade were used as received. All other chemicals, reagents and solvents were of analytical grade and used as received without further purification.

Synthesis of ZnO nanostructures

For the synthesis of ZnO nanostructures, 10 mmol of zinc nitrate ($Zn(NO_3)_2 \cdot 6H_2O$) and 20 mmol of NaOH were dissolved separately in 15 mL of distilled water respectively. The NaOH solution was dropwise added to zinc nitrate solution with constant stirring. To this mixture separately prepared EDA solution (0.5 mL in 20 mL distilled water) was added dropwise and the stirring was continued for 15 min. The whole mixture was then transferred to a stainless steel autoclave containing a 100 mL Teflon container. The autoclave was sealed properly and heated at 180 °C for 2 h in an electric oven. After completion of the reaction the autoclave was naturally cooled down to room temperature. The obtained reaction mass was washed with deionised water in order remove the excess NaOH and unreacted precursor. Then a final wash was given with ethanol. The sample was dried at 80 °C in a vacuum oven for 1 h, and the dried sample was ground in a mortar and pestle and used as such for further analysis and to evaluate its catalytic activity study.

Characterization

The prepared ZnO nanostructures were characterized with different spectroscopic and microscopic techniques. The phases were identified using a powder XRD technique (Bruker AXS model D-8, 10 to 70° range, scan rate = 10° min^{-1}) equipped with a monochromator and Ni-filtered Cu K_α (1.5406 Å) radiation. The as synthesised ZnO nanostructures were studied morphologically using FESEM (HITACHI S-4800). Microstructure analyses were carried out using a field emission transmission electron micrograph (FETEM) performed using a JEOL JEM-2200 FS microscope operating at 200 kV. ^{1}HNMR spectra of organic compounds were recorded on a Varian 400 MHz NMR spectrophotometer with $CDCl_3$ or DMSO-d_6 as a solvent. Coupling constants (J) are given in Hertz. Melting points were determined on a Buchi M-560. Mass spectral data were obtained from LC-MS (Shimadzu 2010). The reaction was monitored by thin layer chromatography (TLC) on Merck's silica gel plates (60 F_{254}). Photoluminescence spectra (PL) were recorded by the photoluminescence spectrometer ShimadzuRF-5301.

Synthesis of benzoxanthene

In a 25 mL round bottom flask a stoichiometric mixture of β-naphthol (1.0 mmol), aromatic aldehydes (1.0 mmol) and 1,3 dicarbonyl compound (dimedone) (1.0 mmol) were mixed together with a catalytic amount (5 mol%) of ZnO in the presence of ethanol : water (5 mL) and refluxed for 1–2 h.

The progress of the reaction was monitored by TLC (30% hexane/ethyl acetate). After completion of the reaction, the catalyst was filtered and the resulting product was extracted with ethyl acetate, dried over anhydrous sodium sulfate and the solvent was evaporated under reduced pressure. The crude product was purified by silica column chromatography using hexane/ethyl acetate (90 : 10 v/v) as an eluent. Proton chemical shifts (δ) are relative to TMS ($\delta = 0$) as an internal standard and expressed in ppm. Coupling constants (J) are given in Hertz. The characterization data, physical constants and NMR of these compounds were found to be identical with those reported in the literature (Table S1, ESI†).

Synthesis of pyranopyrazole

In a 25 mL round bottom flask, ethyl acetoacetate (1.0 mmol), hydrazine hydrate (1.0 mmol), aldehyde (1 mmol), and malononitrile (1 mmol) were mixed together and a catalytic amount (5 mol%) of ZnO was added in the presence of aq. ethanol (5 mL). The reaction was stirred at room temperature for 15–30 min,

The progress of the reaction was monitored by TLC (30% hexane/ethyl acetate). After completion of the reaction, the catalyst was filtered and the resulting product was extracted with ethyl acetate, dried over anhydrous sodium sulfate and the solvent was evaporated under reduced pressure. The crude product was purified by silica column chromatography using hexane/ethyl acetate (Table S2, ESI†).

Results and discussion

In order to investigate the crystalline phases, the synthesized ZnO was analysed with the XRD technique and the XRD pattern is depicted in Fig. 1. The intense XRD peaks confirm the formation of highly crystalline ZnO. The observed XRD peaks at 2θ = 31.7, 34.4, 36.2, 47.6, 56.7, and 62.8° are attributed to (hkl) planes (100), (002), (101), (102), (110) and (103) respectively. The peak positions validate the formation of crystalline ZnO having a hexagonal wurtzite phase. XRD matches with the reported ZnO pattern (JCPDS No. 36-1451) indicating high phase purity and crystallinity. The average crystallite size calculated using Scherer's equation is found to be 30 nm. The observed lattice constants of the prepared ZnO nanostructure having hexagonal wurtzite phase are $a = b = 3.24$ Å and $c = 5.20$ Å. After confirming the crystalline ZnO, further morphological study of a ZnO nanostructure by FESEM and TEM analysis was performed.

FESEM analysis

The morphological study of the prepared ZnO nanostructures was carried out using the FESEM technique and the images are presented in Fig. 2. FESEM analysis indicates the formation of

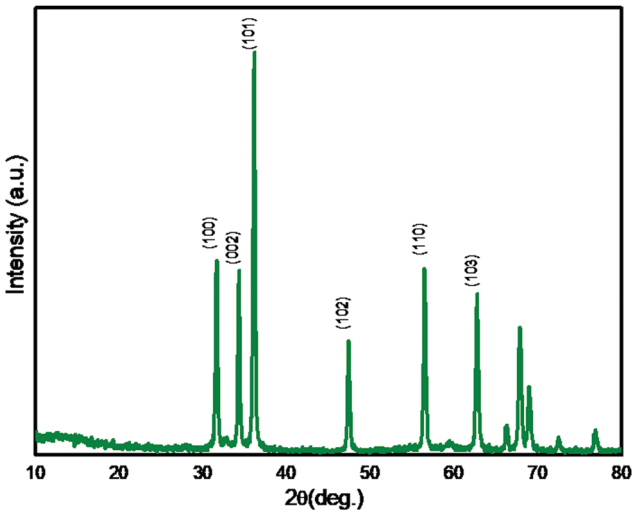

Fig. 1 XRD pattern of ZnO nanostructures.

submicron sized spherical shape marigold flower like hierarchical morphology having a size in the range of 1 to 1.5 μm.

This hierarchical ZnO flower is made up of small nanosized petals having very thin nanosheets of thickness 10–12 nm and along with the flower like morphology, hexagonal shaped plate and nanorods with 50 to 100 nm thickness were also observed. But these nanorods and plates are very few as compared to flowers. The use of EDA leads to the formation of a flower like morphology as it forms a complex with zinc ions (Zn–EDA) and restricts the existence of free zinc ions in solution resulting in controlled formation of zinc nuclei. At higher temperature during the reaction the controlled decomposition of this complex leads to the formation of particular shaped morphology; a detailed mechanism study is in progress.

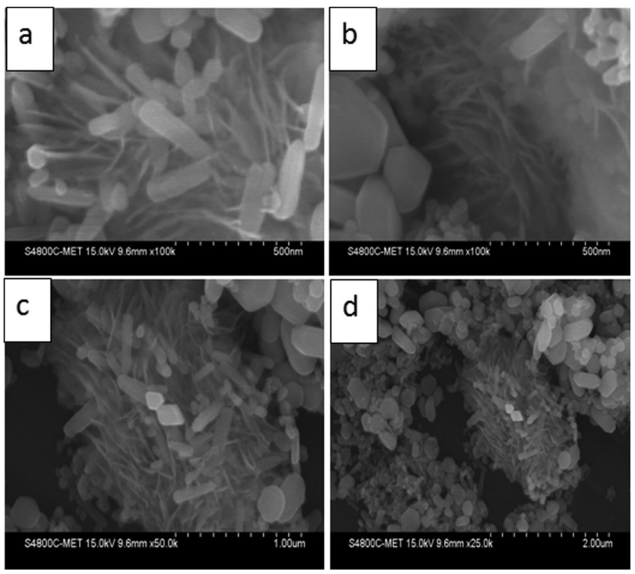

Fig. 2 FESEM of ZnO nanostructures with different resolutions (reaction conditions 180 °C for 2 h).

TEM analysis

TEM micrographs of the as synthesized hierarchical ZnO nanostructures along with the selected area diffraction pattern (SAED) are shown in Fig. 3.

TEM micrographs of ZnO nanostructures prepared at 180 °C for 2 h showed formation of hexagonal, spherical and petal like mixed phase morphology. (TEM image a and b). SAED shown in the inset of Fig. 3b indicates the formation of highly crystalline hexagonal wurtzite phase ZnO nanostructures. The high resolution TEM (HRTEM) image indicates an inter planar spacing of 0.262 nm corresponding to the [002] plane. From the TEM images it can be seen that the flowers are formed *via* self-assembling of very thin nanopetals which are created by self-alignment of tiny ZnO nanostructures. The concentric fused rings can be observed in the SAED pattern and match with the hexagonal phase of ZnO, thereby supporting XRD analysis (inset of Fig. 3b).

Growth mechanism for ZnO nanostructures

The growth mechanism for the formation of ZnO nanostructures is proposed and may follow the following pathways (Scheme 3a–d). During a hydrothermal reaction, the precursors slowly mixed and decomposed into tiny nuclei of ZnO (Scheme 3a and b). Primarily, tiny nuclei of ZnO are formed in the supersaturated solution and further growth of nanoparticles takes place with time (Scheme 3c). Under the optimized reaction conditions (180 °C/hydrothermal, 2 h & EDA), the ZnO nuclei were grown to form hierarchical (hexagonal, spherical and petal like mixed phase morphology) ZnO nanostructures.

The room temperature PL spectrum of the ZnO nanostructures was obtained with an excitation wavelength of 350 nm and is shown in Fig. S7 (ESI†). It shows two distinct peaks at 392 and 490 nm, the sharp and strong ultra violet emission peak at 392 nm corresponds to band edge emission and the broad emission peak centered at 490 nm is observed due to oxygen vacancies in the ZnO lattice.[39]

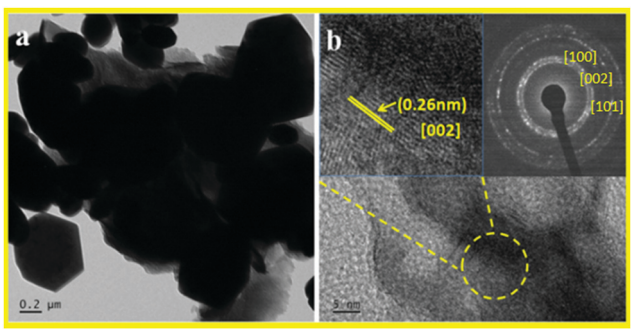

Fig. 3 TEM micrographs of ZnO nanostructures and SAED image (inset of (b), 180 °C for 2 h).

Synthesis of benzoxanthene and pyranopyrazole derivatives

We initially optimized the reaction conditions for the multi-component reaction of β-naphthol, benzaldehyde and dimedone to afford the corresponding benzoxanthene derivative. The various reaction parameters comprising amount of catalyst, influence of solvent and temperature were evaluated for the reactions.

Screening of catalyst

To establish the general reaction conditions for the synthesis of benzoxanthenes, a model reaction of β-naphthol, *p*-nitrobenzaldehyde and dimedone was studied with and without ZnO nanostructured material as a catalyst and the results are summarized in Table 1. The reaction was sluggish and did not proceed in the absence of catalyst even after prolonged reaction time. The use of ZnO nanostructured material afforded good yield of the desired benzoxanthenes.

In order to find the appropriate concentration of ZnO for synthesis, the amount of catalyst varied from 0.5 mol% to 10 mol%, and the results are depicted in Table 1. With increase in catalyst amount the yield of the reaction increases from 65% to 92% respectively. With a higher catalyst amount (>5 mol%) the yield of the product was around 94% this indicates that there was not much increase in the yield. The increase in the catalyst amount did not show any significant improvement in the yield of the resultant product. Based on the above observations 5 mol% catalyst was used for the synthesis of benzoxanthene derivatives.

Screening of solvent

The effect of various solvents on the yield of benzoxanthene was also explored using 5 mol% ZnO nanostructured material and the results are summarized in Table 2.

When the reaction was carried out in water it afforded the desired product in lower yields (20%). After extended reaction time this may due to the inhomogeneity of the reactants. It was observed that the yield of benzoxanthenes in aqueous ethanol (50%) was almost more than 92% whereas, in methanol it was 85%. Other polar aprotic solvents (CH_3CN, DCM, THF, $CHCl_3$, DMF) afforded moderate yield (Table 2, entry 4 to 9), while a non-polar solvent (Table 2, entry 10) resulted in the desired product in lower yield, which required longer reaction time.

Table 1 Optimization of amount of catalyst

Entry	ZnO (*x* mmol)	Yield[a] (%)
1	0.5	65
2	1.0	78
3	2.5	85
4	5.0	92
5	7.5	94
6	10.0	94

[a] Isolated yield after chromatographic separation. Reaction conditions: aldehyde (1 mmol), 2-naphthol (1 mmol), 1, 3 dicarbonyl compound (1 mmol), catalyst (5 mol%) were stirred in 5 mL ethanol : water at reflux temperature for 1–2 h.

Table 2 Effect of solvent

Entry	Solvent	Time	Yield[a] (%)
1	H_2O	6 h	>20
2	EtOH : H_2O	60 min	92
3	MeOH	90 min	85
4	CH_3CN	60 min	89
5	DCM	75 min	80
6	THF	60 min	82
7	$CHCl_3$	60 min	86
9	DMF	90 min	65
10	Toluene	120 min	55

[a] Isolated yield after chromatographic separation. Reaction conditions: aldehyde (1 mmol), 2-naphthol (1 mmol), 1,3 dicarbonyl compound (1 mmol), catalyst (5 mol%) were stirred in 5 mL solvent ethanol : water at reflux temperature.

Among the studied solvents aqueous ethanol (50%) gave an excellent yield of benzoxanthene within 1–2 h of reaction time. For further investigation we used 5 mol% of catalyst and aqueous ethanol (50%) as a solvent system.

Effect of temperature

The effect of temperature was studied by carrying out the control reaction at room temperature and under reflux temperature in the presence of nanostructured ZnO and aqueous ethanol as a solvent. The best result was obtained at reflux temperature (78–80 °C). At room temperature (25–27 °C) the reaction did not proceed even after prolonged reaction time.

To explore the further applicability of this reaction using the optimized reaction conditions, we extended the methodology for the synthesis of diverse derivatives of benzoxanthene using various aromatic aldehydes with either electron-releasing or electron-withdrawing substituents in the *ortho, meta* and *para* positions (Scheme 1), and the results are summarized in Table 3.

The benzaldehyde and halogenated benzaldehydes gave almost more than 87% yield (Table 3, entries **4a**, **4b**, **4e**, **4i**). 4-Nitrobenzaldehyde afforded 92% yield of the corresponding benzoxanthene in a shorter time (Table 3, entry **4c**). It was observed that the reaction proceeds at a faster rate with all the aldehydes possessing electron-withdrawing groups on the aromatic ring than aldehydes possessing electron-donating substituents (Table 3, entries **4d**, **4f**, **4g**, **4h** & **4j**) giving good to excellent yield of the corresponding products.

After effective application of ZnO nanostructures as a heterogeneous catalyst for the synthesis of benzoxanthene derivatives we further extended the methodology for multi-component synthesis of pyranopyrazole derivatives. (Scheme 2).

The multi-component reaction of aromatic aldehydes with ethylacetoacetate, hydrazine hydrate and malononitrile in the presence of ZnO nano structures as a heterogeneous catalyst is

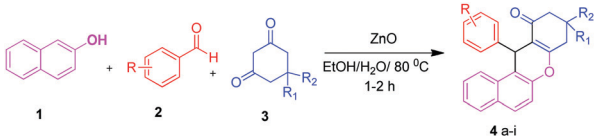

Scheme 1 ZnO catalysed synthesis of benzoxanthene.

Table 3 Synthesis of benzoxanthenes

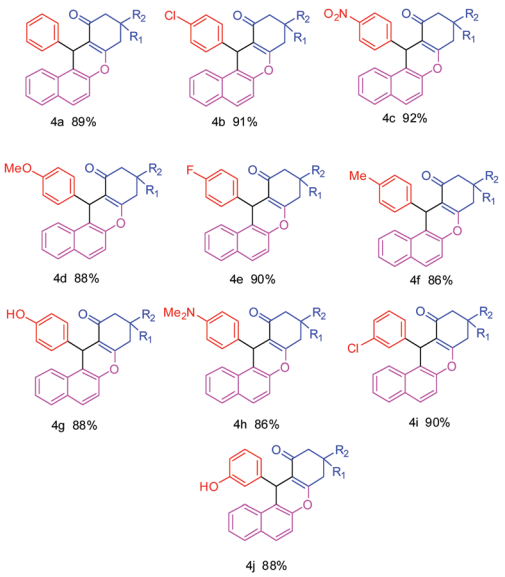

Reaction conditions: Isolated yield after chromatographic separation. Reaction conditions: aldehyde (1 mmol), 2-naphthol (1 mmol), 1,3 dicarbonyl compound (1 mmol), catalyst (5 mol%) were stirred in 5 mL ethanol–water at reflux temperature for 1–2 h.

described under optimized reaction with respect to the amount of catalyst and solvent as mentioned in Scheme 1.

To optimize the reaction conditions, the model reaction was studied with 4-chlorobenzaldehyde, ethyl acetoacetate, malononitrile and hydrazine hydrate. Various solvents were studied for the optimization of the reaction conditions and the best results were obtained with ethanol–water at room temperature. A wide range of aromatic aldehydes were successfully converted to the analogous pyranopyrazole derivatives under the optimized reaction conditions. It was found that the ZnO nano structured material effectively catalyzes the reaction within 15–30 min at room temperature affording good to excellent yield of the corresponding derivatives. These results are depicted in Table 4.

Unsubstituted aromatic aldehyde (benzaldehyde) afforded 90% yield (Table 4, entry **5a**); however amongst the halogenated aldehydes, 4-chlorobenzaldehyde (Table 4, entry **5b**) furnished 98% yield of the resultant pyranopyrazole derivative within 10 min of reaction time, whereas other halogenated aldehydes afforded more than 90% yield (Table 4, entries **5e** and **5i**). The reaction of 4-nitrobenzaldehyde was completed within 10 min giving 94% yield of the corresponding product (Table 4, entry **5c**). Aldehydes having electron releasing groups also reacted within 15–30 min with good to excellent yield

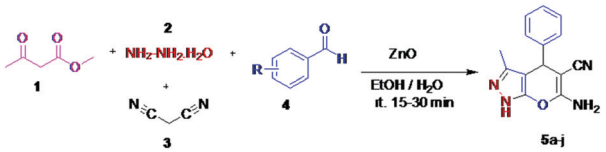

Scheme 2 ZnO catalysed synthesis of pyranopyrazole.

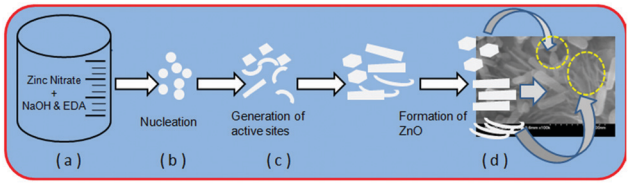

Scheme 3 Plausible growth mechanism of ZnO nanostructures ((d) is the FESEM image of the ZnO nanostructures).

Table 4 Synthesis of pyranopyrazole derivatives

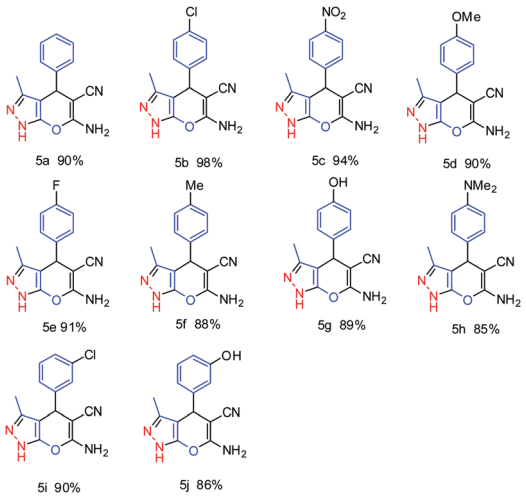

Reaction conditions: Isolated yield after chromatographic separation. Reaction conditions: ethyl acetoacetate (1.0 mmol), hydrazine hydrate (1.0 mmol), aldehyde (1 mmol), malononitrile (1 mmol) were stirred in ethanol–water for 10–15 min at room temperature, catalyst (5 mol%).

(85–90%) of pyranopyrazole derivatives. (Table 4 entries **5d**, **5g** and **5j**). It was observed that the majority of reactions proceed at a faster rate with ZnO nanostructured material at room temperature. Das *et al.* have reported nano crystalline ZnO (10 mol%) catalyzed one pot multicomponent reactions for the synthesis of pyranopyrazole derivatives in water : ethanol at room temperature affording 83 to 98% yield in 3 h.[40]

Recycling study

The reusability of the catalyst was also studied under the optimized reaction conditions. After completion of the reaction the catalyst was recovered, filtered and washed repeatedly with ethyl acetate and dried.

It was reused under the optimized reaction conditions and it was found that the yields of benzoxanthene and pyranopyrazole were almost comparable. The catalyst recovered after the first cycle was used for the subsequent four cycles and the yield of the corresponding product obtained in each cycle is summarized in Table 5. It was observed that the % yield of these derivatives was negligibly lowered even after five cycles. These observations suggest that the catalyst surface remains active during successive cycles. Although the slight decrease in the catalytic activity of ZnO might be

Table 5 Reusability of the catalyst

Entry	Number of cycles	Yield[a] (%)
1	Fresh	95
2	First	92
3	Second	89
4	Third	85
5	Fourth	80
6[b]	Fifth	94

[a] Isolated yield. [b] Used catalyst from fourth recycle, heated at 150 °C for 60 min in a N_2 atmosphere. Reaction conditions: 1 : 1 : 1 mmol reactant with catalyst (5 mol%) were stirred in 5 mL ethanol.

due to the deactivation of the active sites of the catalyst. Also, control experimental study of a commercial ZnO sample (bulk size) with as synthesized ZnO nanostructures was carried out. In comparison with the as-synthesized ZnO nanostructures the commercial ZnO sample (bulk size) shows 40 to 50% less reaction yields.

Plausible reaction mechanism for the synthesis of benzoxanthene

A plausible reaction mechanism for the synthesis of benzoxanthene derivatives using hierarchical ZnO nanostructures is illustrated in Scheme 4. Hierarchical ZnO nanostructure coordinate with carbonyl oxygen and enhance the electrophilicity of the carbonyl carbon of aldehydes (**1**) followed by subsequent attack of dimedone to give an alkene intermediate (**2**). The nucleophilic attack of an oxygen atom of β-naphthol (**3**) to the electron deficient intermediate (**2**) affords intermediate (**4**). The subsequent elimination of hydrogen followed by a water molecule (**5–6**) results in the desired benzoxanthene derivatives (**7**).

Plausible reaction mechanism for the synthesis of pyranopyrazole

Ethyl acetoacetate is activated by ZnO nanostructures followed by attack of hydrazine, which results in the formation of pyrazolone, intermediate (i). Also, the carbonyl group of aldehyde is activated by nanostructured ZnO and then it undergoes Knoevenagel condensation with malononitrile to afford intermediate (ii). The interaction between intermediate (i) and intermediate (ii) enables Michael addition type reaction. The intramolecular cyclization followed by tautomerization gives the corresponding pyranopyrazole derivatives (iii) (Scheme 5).

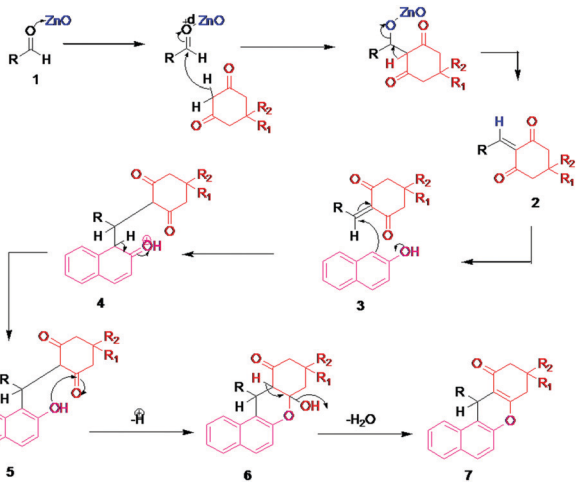

Scheme 4 Proposed reaction mechanism for the synthesis of benzoxanthene derivatives.

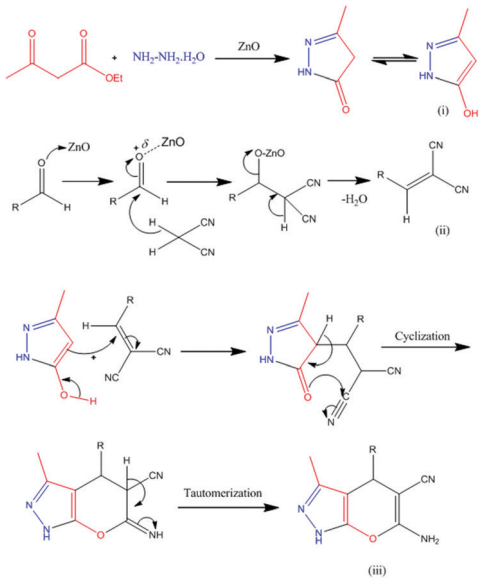

Scheme 5 Proposed reaction mechanism for the synthesis of pyranopyrazole derivatives.

Conclusions

In a nutshell, we have successfully used a hydrothermal technique for the synthesis of a highly crystalline hexagonal ZnO nanostructure having spherical and petal like mixed morphology. Furthermore, the effective use of the synthesized hierarchical ZnO nanostructures as a heterogeneous catalyst was evaluated for the synthesis of benzoxanthene and pyranopyrazole derivatives *via* one-pot multi-component reactions in good to high yields under ambient reaction conditions. In addition, the catalyst could be easily recovered by simple filtration and reused for several cycles without significant loss in its catalytic activity.

Conflicts of interest

There are no conflicts to declare.

Acknowledgements

The authors sincerely acknowledge Centre for materials for electronics technology (C-MET) Pune and Haribhai V. Desai College, Pune for characterization. We also thank Ness Wadia

Nanomaterial Research Centre, NowrosjeeWadia College, Pune for providing lab facilities.

References

1 L. Weber, K. Illegen and M. Almstetter, *Synlett*, 1999, 366–374.
2 N. Koukbai, E. Kolvari, A. Khazaei, M. A. Zolfigol, B. Shirmardi-Shaghasemi and H. R. Khavasi, *Chem. Commun.*, 2011, **47**, 9230–9232.
3 J. P. Poupelin, G. Saint-Ruf, O. Foussard-Blanpin, G. Marcisse, G. Uchida-Ernouf and R. Lacroix, *Eur. J. Med. Chem.*, 1978, **13**, 67–71.
4 R. W. Lambert, J. A. Martin, J. H. Merrett, K. E. B. Parkes and G. J. Thomas, *PCT Int. Appl.* WO9706178, 1997.
5 T. Hideo and J. Teruomi (Sankyo Co), *Japan Pat.*, 56005480, 1981.
6 S. M. Menchen, S. C. Benson, J. Y. L. Lam, W. Zhen, D. Sun, B. B. Rosenblum, S. H. Khan and M. Taing, *US Pat.* 6583168, June 24, 2003.
7 C. G. Knight and T. Stephens, *Biochem. J.*, 1989, **258**, 683–687.
8 M. Ahmad, T. A. King, D. K. Ko, B. H. Cha and J. J. Lee, *J. Phys. D: Appl. Phys.*, 2002, **35**, 1473–1476.
9 J. Li, W. Tang, L. Lu and W. Su, *Tetrahedron Lett.*, 2008, **49**, 7117–7120.
10 G. M. Nazeruddin, M. S. Pandharpatte and K. B. Mulani, *Indian J. Chem.*, 2011, **50B**, 1532–1537.
11 K. G. Verma, K. Raghuvanshi, R. K. Verma, P. Dwivedi and M. S. Singh, *Tetrahedron*, 2011, **67**, 3698–3704.
12 G. C. Nandi, S. Samai, R. Kumar and M. S. Singh, *Tetrahedron*, 2009, **65**, 7129–7134.
13 Y. B. Shen and G. W. Wang, *ARKIVOC*, 2008, **xvi**, 1–8.
14 B. Das, P. Thirupathi, K. Ravinder Reddy, B. Ravikanyh and L. Nagarapu, *Catal. Commun.*, 2006, 737–742.
15 T. S. Jin, J. S. Zhang, A. Q. Wang and T. S. Li, *Ultrason. Sonochem.*, 2006, **13**, 220–224.
16 T. S. Jin, J. S. Zang, J. C. Xiao, A. Q. Wang and T. S. Li, *Synlett*, 2004, 866–870..
17 H. N. Karade, M. Sathe and M. P. Kaushik, *ARKIVOC*, 2007, **xiii**, 252–258.
18 M. Kidwai, K. Singhal and S. Kukreja, *Can. J. Chem.*, 2008, **86**, 799–802.
19 S. Kantevari, R. Bantu and L. Nagarapu, *ARKIVOC*, 2006, **xvi**, 136–148.
20 G. P. Ellis, *The Chemistry of Heterocyclic Compounds. Chromenes, Chromanes and Chromones*, ed. A. Weissberger and E. C. Taylor, John Wiley, New York, 1977, ch. 11, p. 11.
21 E. A. Hafez, M. H. Elnagdi, A. G. A. Elagemey and F. M. A. A. El-Taweel, *Heterocycles*, 1987, **26**, 903–907.
22 M. A. Sofan, F. M. A. A. El-Taweel and M. H. Liebigs Elnagdi, *Ann. Chem.*, 1989, 935–936.
23 A. Galil, F. B. Riad, S. Sherif and M. Elnagdi, *Chem. Lett.*, 1982, 1123–1126.
24 M. Kidwai, S. Saxena, M. Khan and S. Thukral, *Bioorg. Med. Chem. Lett.*, 2005, **15**, 4295–4298.
25 J. Li, L. Lu and W. Su, *Tetrahedron Lett.*, 2010, **51**, 2434–2437.
26 J. M. Khurana and D. Magoo, *Tetrahedron Lett.*, 2009, **50**, 4777–4780.
27 Q. Zhang, H. Su, J. Luo and Y. Wei, *Green Chem.*, 2012, **14**, 201–208.
28 P. Ghosh and A. Das, *J. Org. Chem.*, 2013, **78**, 6170–6181.
29 K. Kong, H. L. Wang, D. Fang and Z. L. Liu, *Catal. Commun.*, 2008, **9**, 650–673..
30 N. Sakai, G. K. Prasad, Y. Ebina, K. Takada and T. Sakai, *Chem. Mater.*, 2006, **18**, 3596–3598.
31 D. Shao, M. Yu, H. Sun, T. Hu, J. Lian and S. Swayer, *Nanoscale*, 2013, **5**, 3664–3667.
32 P. S. Mane, W. J. Lee, H. M. Pathan and S. H. Han, *J. Phys. Chem. B*, 2005, **109**, 24254–24259.
33 N. Madhusudhana, K. Yogendra and K. M. Mahadevan, *Res. J. Chem. Sci.*, 2012, **2**(5), 72–77.
34 O. Seven, B. Dindar, S. Aydemir, D. Metin, M. A. Ozinel and S. Icli, *J. Photochem. Photobiol., A*, 2004, **165**, 103–107.
35 D. G. Kumbhar, V. U. Pandit, S. D. Deshmukh, J. D. Ambekar, S. S. Arbuj and S. B. Rane, *J. Nanoeng. Nanomanuf.*, 2015, **5**, 227–231.
36 V. U. Pandit, S. S. Arbuj, R. Hawaldar, P. V. Kshirsagar, U. P. Mulik, S. W. Gosavi, C. J. Park and B. B. Kale, *J. Mater. Chem. A*, 2015, **3**, 4338–4344.
37 V. U. Pandit, S. S. Arbuj, U. P. Mulik and B. B. Kale, *Environ. Sci. Technol.*, 2014, **48**, 4178–4183.
38 V. U. Pandit, S. S. Arbuj, Y. B. Pandit, S. D. Naik, S. B. Rane, U. P. Mulik, S. W. Gosawi and B. B. Kale, *RSC Adv.*, 2015, **5**, 10326–10331.
39 S. S. Arbuj, N. Rumale, A. Pokle, J. D. Ambekar, S. B. Rane, U. P. Mulikand and D. P. Amalnerkar, *Sci. Adv. Mater.*, 2014, **6**, 269–275.
40 P. Bhattacharyya, K. Pradhan, S. Paul and A. R. Das, *Tetrahedron Lett.*, 2012, **53**(35), 4687–4691.